

Model for the spatio-temporal intermittency of the energy dissipation in turbulent flows

Fabio Lepreti,* Vincenzo Carbone, and Pierluigi Veltri

*Dipartimento di Fisica, Università della Calabria,
Via P. Bucci 31/C, I-87036 Rende (CS), Italy and
Consorzio Nazionale Interuniversitario per le Scienze
Fisiche della Materia (CNISM), Unità di Cosenza, Italy*

(Dated: October 1, 2018)

Abstract

Modeling the intermittent behavior of turbulent energy dissipation processes both in space and time is often a relevant problem when dealing with phenomena occurring in high Reynolds number flows, especially in astrophysical and space fluids. In this paper, a dynamical model is proposed to describe the spatio-temporal intermittency of energy dissipation rate in a turbulent system. This is done by using a shell model to simulate the turbulent cascade and introducing some heuristic rules, partly inspired by the well known p -model, to construct a spatial structure of the energy dissipation rate. In order to validate the model and to study its spatially intermittency properties, a series of numerical simulations have been performed. These show that the level of spatial intermittency of the system can be simply tuned by varying a single parameter of the model and that scaling laws in agreement with those obtained from experiments on fully turbulent hydrodynamic flows can be recovered. It is finally suggested that the model could represent a useful tool to simulate the spatio-temporal intermittency of turbulent energy dissipation in those high Reynolds number astrophysical fluids where impulsive energy release processes can be associated to the dynamics of the turbulent cascade.

PACS numbers: 47.27.Eq, 02.50.Ey, 47.53.+n

*Corresponding author. Email address: lepreti@fis.unical.it

I. INTRODUCTION

The dynamics of fluids and plasmas, both in laboratory experiments and in astrophysical or geophysical systems, is very often characterized by the presence of turbulent motions [1, 2]. In several contexts of astrophysics and space physics, it is extremely important to model some of the effects related to the turbulent dynamics. In particular, describing in a proper way the spatio-temporal intermittency of the turbulent energy dissipation process is one of the basic ingredients for the study of several astrophysical systems. As relevant examples, we can consider the active regions of the solar corona [3, 4], the interstellar medium [5], and accretion disks [6].

Intermittency is one of the most investigated problems in the field of fully developed turbulence (see [1] and references therein). Among the many approaches used for the study of intermittency in turbulence, here we want to briefly recall only some of them, which are related to the work presented in this paper. A number of random cascade models (see *e.g.* [7, 8, 9, 10]) were initially proposed to reproduce the observed intermittency corrections (see *e.g.* [11]) to the scaling laws of the classical Kolmogorov theory of turbulence [12]. Another interesting approach to the modeling of intermittency of the turbulent energy cascade is based on the use of dynamical deterministic models known as shell models (see the reviews by Bohr et al. [13], Giuliani [14], Biferale [15]). More recently, several relevant developments have led to a beginning of a deeper understanding of the intermittency phenomenon. To mention but a few: the role of Lagrangian conservation laws [16] and nonlocal interactions [17] on intermittency, and the introduction of new multifractal approaches for the description of velocity increments statistics [18].

Besides these important theoretical advances, there are several more specific situations where a simple dynamical system modeling of the intermittency in the turbulent cascade can be extremely helpful. This can be the case of astrophysical and space fluids, where, due to the extremely large Reynolds numbers, dynamical models which are able to simulate the turbulent cascade and the related energy dissipation processes in Reynolds number regimes which are not far from the real ones (at least with respect to direct numerical simulations) can represent an essential ingredient for the modeling of such physical systems. An example is given by the recent applications of shell models to the description of the statistical properties of solar flares [19, 20], and to the nanoflares occurring in solar coronal loops [21]. In this

framework, it is worth to point out that shell models provide only a temporal description of the intermittency properties since they lack any spatial information. The possibility to have a dynamical “shell-like” model capable of reproducing some intermittency properties both in space and time would thus be attractive.

For the reasons explained above, in this work we propose a simple method to model the intermittent character of energy dissipation in a turbulent system in both space and time, by using a shell model together with some rules inspired to some extent by the well known turbulence p -model [10]. The paper is organized as follows. In Section II we recall the main ideas concerning shell models and the p -model, in Section III we give a description of the proposed method, in Section IV we provide some details about the numerical procedure, in Section V we show the results of the spatially intermittency analysis performed in order to validate the proposed model, while the conclusions are drawn in Section VI.

II. BACKGROUND

A. Shell model

Shell models were introduced in 70’s by Obukhov [22], Gledzer [23], and Desnyansky and Novikov [24] in the context of hydrodynamic turbulence and, since then, used extensively both in hydrodynamics (see e.g. [25, 26]) and magnetohydrodynamics (MHD) (see e.g. [27, 28, 29, 30]). They are based on a set of coupled nonlinear ordinary differential equations which describe the dynamics of the turbulent energy cascade in the wave-vector space. The dynamical and statistical behavior of shell models have been investigated in detail in many works (see [13, 14, 15] and references therein) and it has been shown that they are able to describe several properties of the turbulent energy cascade process. The main advantage of shell models is that they can be investigated through numerical simulations at high Reynolds numbers much more easily than Navier-Stokes (N-S) or MHD equations, due to the reduced number of degrees of freedom. On the other hand, an obvious minus of these models is the absence of any information about spatial structures.

Shell models are built up by dividing the wavevector space in a discrete number of shells of radius $k_n = k_0 \lambda^n$, with $\lambda > 1$ fixing the shell logarithmic spacing (usually $\lambda = 2$) and $n = 1, 2, \dots, N$. Each shell is associated with a dynamical complex variable $u_n(t)$ which

represents the time evolution of velocity fluctuations at scale $\ell_n \sim k_n^{-1}$. The evolution equations for the variables $u_n(t)$ are written by introducing nonlinear terms in the form of quadratic couplings between neighbouring shells. The coupling coefficients are chosen to satisfy scale invariance and the conservation of the ideal invariants, as for example the total energy and the kinetic helicity for N-S equations.

For this work we use the hydrodynamic shell model proposed by L'vov et al. [31], also known as Sabra model. The evolution equations of the shell variables are

$$\begin{aligned} \frac{du_n}{dt} = & ik_n \left(u_{n+2}u_{n+1}^* - \frac{1}{4}u_{n+1}u_{n-1}^* + \frac{1}{8}u_{n-1}u_{n-2} \right) \\ & - \nu k_n^2 u_n + f_n, \end{aligned} \quad (1)$$

where ν represents the kinematic viscosity, and f_n is a forcing term usually acting on some low wavenumber shells. From Eq. (1), we can derive the evolution equation for the n -th shell kinetic energy $E_n = (u_n u_n^*)/2$:

$$\frac{dE_n}{dt} = -\Pi_n - 2\nu k_n^2 E_n + \Re(u_n^* f_n), \quad (2)$$

where

$$\begin{aligned} \Pi_n = k_n \Im & \left(u_n^* u_{n+2} u_{n+1}^* + \frac{1}{4} u_n u_{n+1}^* u_{n-1} \right. \\ & \left. + \frac{1}{8} u_n^* u_{n-1} u_{n-2} \right) \end{aligned} \quad (3)$$

gives the kinetic energy flux through the n -th shell (the symbols \Re and \Im denote the real and imaginary parts respectively of a complex number).

The total energy dissipation rate $\varepsilon(t)$ can be defined as

$$\varepsilon(t) = \nu \sum_{n=1}^N k_n^2 |u_n|^2. \quad (4)$$

B. The p -model

The p -model has been designed to describe the observed multifractal behavior of the energy dissipation rate in fully turbulent flows [10]. Without loss of generality, in this paper we consider, for simplicity, a one-dimensional spatial domain. In this case, the total dissipation rate $\varepsilon_r(x)$ in the segment $[x, x+r]$ is equal to $\varepsilon_r(x) = \int_x^{x+r} \varepsilon(x) dx$, $\varepsilon(x)$ being the energy dissipation rate in the x position. In the p -model, an interval of size r breaks

down into two subintervals of size $r/2$, and the energy flux to these smaller eddies proceeds unequally. A fraction p (with $0.5 \leq p \leq 1$) of the dissipation contained in the parent interval is distributed equally on one of the two subintervals (left or right with equal probability), and the remaining $(1 - p)$ fraction on the other subinterval. This process starts from the integral scale L (where we have only one interval) and is repeated until segments of size η (corresponding to the dissipative scale) are created. It has been shown in Ref. [10] that using $p = 0.7$ the multifractal spectrum of the synthetic dissipation signal obtained through the p -model reproduces extremely well the results of experiments.

III. THE MODEL

In a few words, the basic idea of the method proposed here consists in using a shell model to describe the dynamics of the turbulent cascade process and in providing a spatial structure to the energy dissipation using some rules, which partly recall the p -model, to distribute in space the energy fluxes given by the shell model.

We consider a one-dimensional spatial domain whose size is denoted by L . As a base for the construction of the spatial energy structure we use a hierarchy of N scales $\ell_n = 2^{1-n}L$ ($n = 1, 2, \dots, N$). For each scale n we can define a set of 2^{n-1} disjoint segments of size ℓ_n which cover the spatial domain. Let us note that this is the same hierarchical structure as in the p -model, that is, each segment at the scale n can be considered as parent of two corresponding segments at the scale $n + 1$ which have half the size and cover the same subinterval as the parent.

Let us now suppose that the N scales of this hierarchy are associated with the N shells of the shell model, and that $\ell_n = 1/k_n$. At each time step t_i ($i=1,2,\dots$) of the numerical solution of the shell model equations, we can calculate the energy increment $\Delta E_n(t_i)$ of the n -th shell as

$$\Delta E_n(t_i) = E_n(t_i) - E_n(t_{i-1}) . \quad (5)$$

These increments are used to construct a spatial energy structure which evolves in time parallelly to the shell model as explained below.

The increments $\Delta E_n(t_i)$ are distributed over the spatial grid of the corresponding scale using the following criteria:

- If $\Delta E_n(t_i) > 0$ we first divide the energy $\Delta E_n(t_i)$ among the segments at the scale $n-1$ (which thus play the role of parent segments) proportionally to the energy contained in them at the scale $n-1$. The energy increment thus obtained for each parent segment is then transferred to the corresponding two daughter segments in the same way as in the p -model, that is, adding a fraction p of the increment ($0.5 \leq p \leq 1$) to one of the daughters (left or right with equal probability) and the remaining $(1-p)$ fraction to the other daughter.
- If $\Delta E_n(t_i) < 0$ the increment is subtracted from the energy at the scale n in such a way that each segment is depleted by a fraction of $\Delta E_n(t_i)$ proportional to the energy content of the segment itself at the same scale.

As a result of the procedure described above, to each one of the 2^{n-1} segments which cover the domain at the scale n is attributed a kinetic energy $E_l^{(n)}(t)$ (where $l = 1, \dots, 2^{n-1}$ is the index denoting the segments at the scale n). The total energy at the scale n equals the kinetic energy of the corresponding shell, that is, $\sum_{l=1}^{2^{n-1}} E_l^{(n)}(t) = |u_n(t)|^2/2$.

In order to have an evolution of the spatial energy structure, the spatial distribution of the p and $(1-p)$ values is changed during the time evolution. Two different methods, described below, were used to perform this changes in time and we denote by Model A and Model B the two versions of the model corresponding respectively to these two methods.

Model A. In the first version of the model the changes of the probabilities in space are done at the same time instant for all the segments at a given scale n . Let us suppose that the last change in the p distribution at the scale n occurs at the time step $t_j^{(n)}$. At each time step t_i we calculate the *instantaneous eddy turnover time* $\tau_e^{(n-1)}(t_i) = [k_{n-1}u_{n-1}(t_i)]^{-1}$ for the scale $n-1$ and compare it to the time elapsed from the last change $\Delta t^{(n)} = t_i - t_j^{(n)}$. If $\Delta t^{(n)} > \tau_e^{(n-1)}$, the p spatial distribution at the scale n is redrawn. This procedure is followed for each $n > 1$.

Model B. In the second version the spatial changes of the probabilities are done independently for the different segments at a given scale n . Indeed one of such changes always involves a couple of segments l and $l+1$ (where l is an odd integer number), because if the probability is p for the segment l it must be $1-p$ for the segment $l+1$ and viceversa. As a consequence, if we denote by $t_j^{(n,l)}$ the last change for the segment l at the scale n , we have that $t_j^{(n,l)} = t_j^{(n,l+1)}$ for a couple of neighbouring segments with l odd integer. At each time step t_i ,

we compute the *local instantaneous eddy turnover time* for the corresponding *father segment* at the scale $n - 1$ (whose index is $l_f = \frac{l+1}{2}$), that is, $\tau_e^{(n-1, l_f)}(t_i) = [k_{n-1} \sqrt{2E_{l_f}^{(n-1)}(t_i)}]^{-1}$ and compare it to the time elapsed from the last change $\Delta t^{(n, l)} = \Delta t^{(n, l+1)} = t_i - t_j^{(n, l)}$. If $\Delta t^{(n, l)} > \tau_e^{(n-1, l_f)}(t_i)$ the probability values are redrawn for the segments l and $l + 1$. This procedure is followed for each $n > 1$.

The two procedures described above aim to describe phenomenologically the correlations arising in the cascade due to the scaling of the eddy turnover times. The main difference between them consists in the fact that in Model B we try to take into account also the local dynamics of the turbulent cascade on the spatial domain.

In both the versions of the model, summing the contribution coming from all the scales, we obtain the spatial shape of the energy density $w(x, t)$ as

$$w(x, t) = \sum_{n=1}^N \frac{E_{l_n(x)}^{(n)}}{\ell_n}, \quad (6)$$

where x denotes the grid position, corresponding to the smallest scale grid spacing, and $l_n(x) = \text{Int}[(x - 1)/\ell_n] + 1$ (Int denotes the integer part of a real number). We can now define also an energy dissipation rate which depends on the spatial coordinate as

$$\varepsilon(x, t) = \nu \sum_{n=1}^N k_n^2 \frac{E_{l_n(x)}^{(n)}}{\ell_n}. \quad (7)$$

IV. NUMERICAL PROCEDURE

The shell model equations Eqs. (1) have been numerically solved using a 4-th order Runge-Kutta scheme. The parameters used in the simulations are $N = 15$, $\nu = 10^{-4}$, $k_0 = 2^{-5}$, and $\lambda = 2$. We used an external forcing term applied on the 3-rd and 4-th shell given by $f_3 = f_4 = 0.1(1 + i)$. With these parameters the Reynolds number is $Re \simeq 10^5$ and the large scale eddy turnover time $\tau_e \simeq 40$. A sample of the total energy dissipation rate $\varepsilon(t)$ given by the shell model is shown in Fig. 1.

The number of grid points in the 1-D spatial domain is 2^{14} . Another free parameter of the model is the p value used to construct the spatial structure of the energy dissipation. It should be clear to the reader that it is not necessary to use the value $p = 0.7$ which allows the p -model to reproduce the multifractal structure of the energy dissipation rate observed in experiments of fully developed turbulence [10]. This is why the models proposed here,

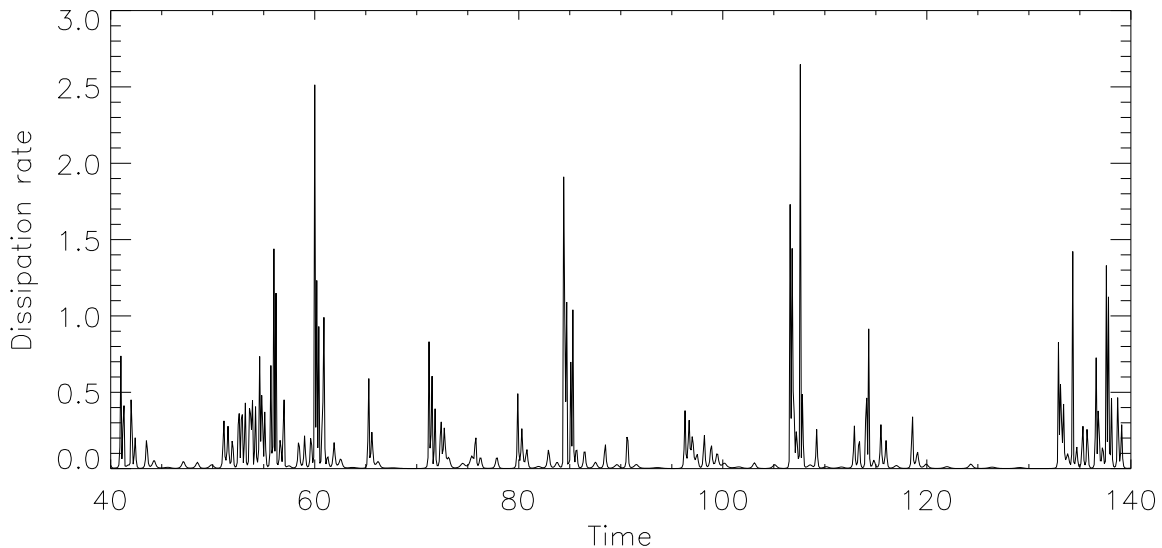


FIG. 1: A sample of the total energy dissipation rate given by the shell model.

although inspired to some extent by the p -model, are substantially different from it, being characterized also by the dynamics provided by the shell model and by the evolution of the p spatial distribution. The multifractal properties of the spatial energy dissipation given by the model change in time. More precise indications about the values to be attributed to the p parameter can be found from the application of the model to well defined physical situations, a question which we plan to further investigate in the future. For this work, we have performed numerical simulations using the values of $p = 0.7, 0.8, 0.9, 1$ for Model A, and $p = 0.7, 0.8$ for Model B. We would like to remark that changing the spatial distribution of the p and $1 - p$ values according to the instantaneous eddy turnover times at each scale, as described in the previous section, is necessary for describing the intermittent behavior of the energy dissipation. As a confirmation, we performed a simple test in which we modified the spatial distribution of the probabilities at each time step and obtained that in this case the energy dissipation rate is not intermittent for any value of p .

V. ANALYSIS OF THE SPATIAL INTERMITTENCY

In order to validate the proposed models, we performed an analysis of the spatial intermittency properties of the energy dissipation rate for different values of the p parameter.

This has been done both by calculating the kurtosis of $\varepsilon(x)$ and by looking for the presence of multifractal scaling laws in $\varepsilon(x)$ [32, 33, 34]. In this way, some comparisons to the scaling exponents of structure functions found in turbulence experiments can also be made.

The starting point for multifractal analysis is the definition of the probability measure

$$\mu_i(r) = \frac{\chi_i(r)}{\chi(L)}, \quad (8)$$

where

$$\chi_i(r) = \int_{S_i(r)} \varepsilon(x) dx. \quad (9)$$

$S_i(r)$ represents a hierarchy of disjoint segments of size r covering the domain L . We can calculate the so called generalized dimensions D_q [35] by looking at the scalings of the q -th order moments of $\mu_i(r)$ vs. r :

$$\langle \mu^q \rangle = \sum_i \mu_i^q(r) \sim r^{(q-1)D_q}. \quad (10)$$

The largest values of q amplify the contribution given to $\langle \mu^q \rangle$ by the most intermittent regions of the measure, while for small values of q the major contribution is due to the most regular regions. If the probability measure is globally self-similar (i.e. non intermittent), D_q is constant and it corresponds to the fractal dimension of the measure. Conversely, if D_q is not constant, the scaling laws are said to be anomalous and the measure can be described as a multifractal object. In this case, it can also be shown that D_q is a nonincreasing function of q [33].

The generalized dimensions D_q can also be related to the scaling exponents ζ_q of the velocity structure functions, which are measured in fluid flows and represent the benchmark for the nonlinear energy cascade modeling. These exponents are defined by

$$\langle \delta v_r^q \rangle = \langle [v(x+r) - v(x)]^q \rangle \sim r^{\zeta_q}. \quad (11)$$

It can be shown [36] that

$$\zeta_q = \frac{q}{3} + \left(\frac{q}{3} - 1 \right) (D_{q/3} - d), \quad (12)$$

where d represents the topological dimension of the support, in our case $d = 1$.

We show in the next two subsection the results obtained for Model A and Model B respectively.

A. Model A

In Fig 2 the space-time structure of the energy dissipation rate $\varepsilon(x, t)$, calculated according to Eq. (7), is shown for $p = 0.8$ and $p = 1$. For the sake of clarity the grey levels refer to the logarithm of $\varepsilon(x, t)$. It can be seen that $\varepsilon(x, t)$ becomes more and more fragmented in space as p increases, as one would expect.

To give a first indication on the intermittency properties of the spatial energy dissipation $\varepsilon(x)$, the time evolution of the kurtosis of $\varepsilon(x)$ for the four different values of p used is shown in Fig. 3. The increase of the typical values of the kurtosis confirms that the level of intermittency is significantly enhanced as p increases from 0.7 up to 1. In Fig. 4 the spatial structure of the energy dissipation rate $\varepsilon(x)$ is shown for four fixed time instants (one for each of the different p values used) where the kurtosis shown in Fig. 3 displays a peak. The four time instants chosen are $t = 73$ for $p = 0.7$, $t = 133$ for $p = 0.8$, $t = 80$ for $p = 0.9$, and $t = 51$ for $p = 1$. This figure shows that at some positions the quantity $\varepsilon(x)$ shows very strong bursts, which appear to become stronger and stronger as p increases.

The multifractal analysis was performed by calculating the moments $\langle \mu^q \rangle$ given in Eq. (10) for $-5 \leq q \leq 5$ at 100 different time instants, namely $t = 41, 42, \dots, 140$. A good scaling region extending almost over the whole r range was found for all the q 's. The generalized dimensions D_q were calculated as averages over all the time instants considered. The plot of D_q vs. q obtained for the four values of p used is shown in Fig. 5. It can be seen that the spectrum of D_q values becomes wider as p increases. This is a consequence of the enhanced level of intermittency which produces stronger and more localized dissipation bursts for larger values of p .

The scaling exponents ζ_q as estimated from the energy dissipation scalings in Model A for the four values of p considered are reported in Table I. As a comparison, the ζ_q exponents computed from a wind tunnel experiment [37] are also shown. It can be seen that Model A gives scaling exponents in agreement with experiments (within the experimental error) for $p \gtrsim 0.9$.

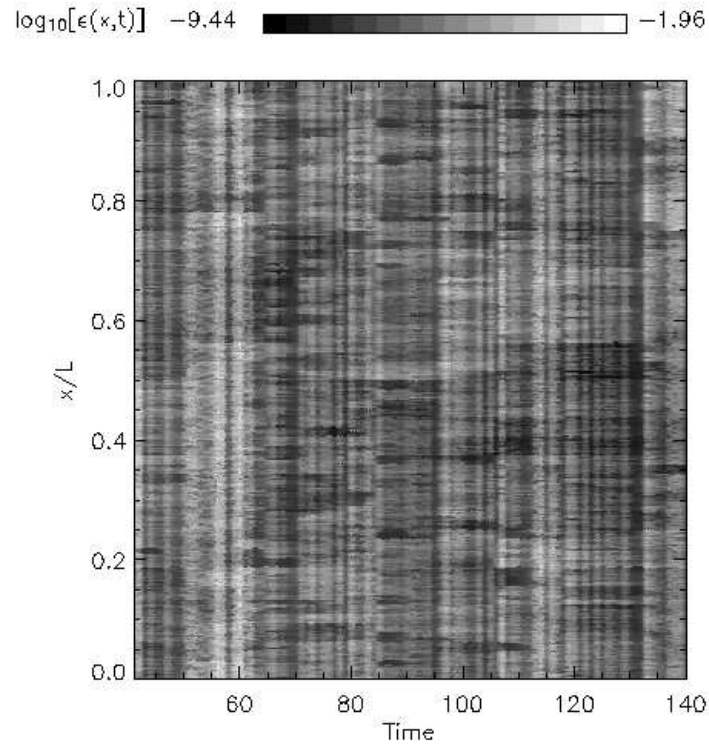
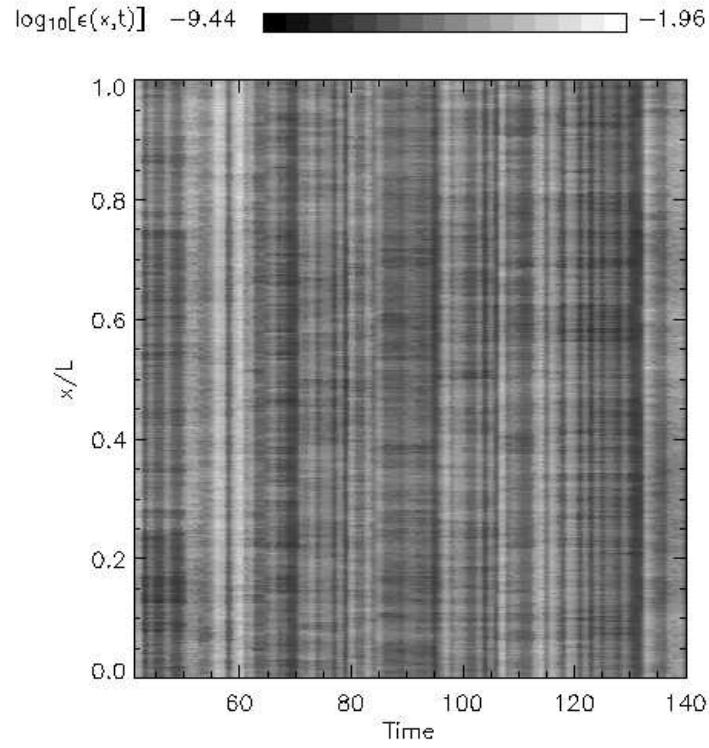


FIG. 2: Space-time structure of the energy dissipation rate $\epsilon(x,t)$ in Model A for $p = 0.8$ (top panel) and $p = 1$ (bottom panel). The grey levels refer to the logarithm of $\epsilon(x,t)$.

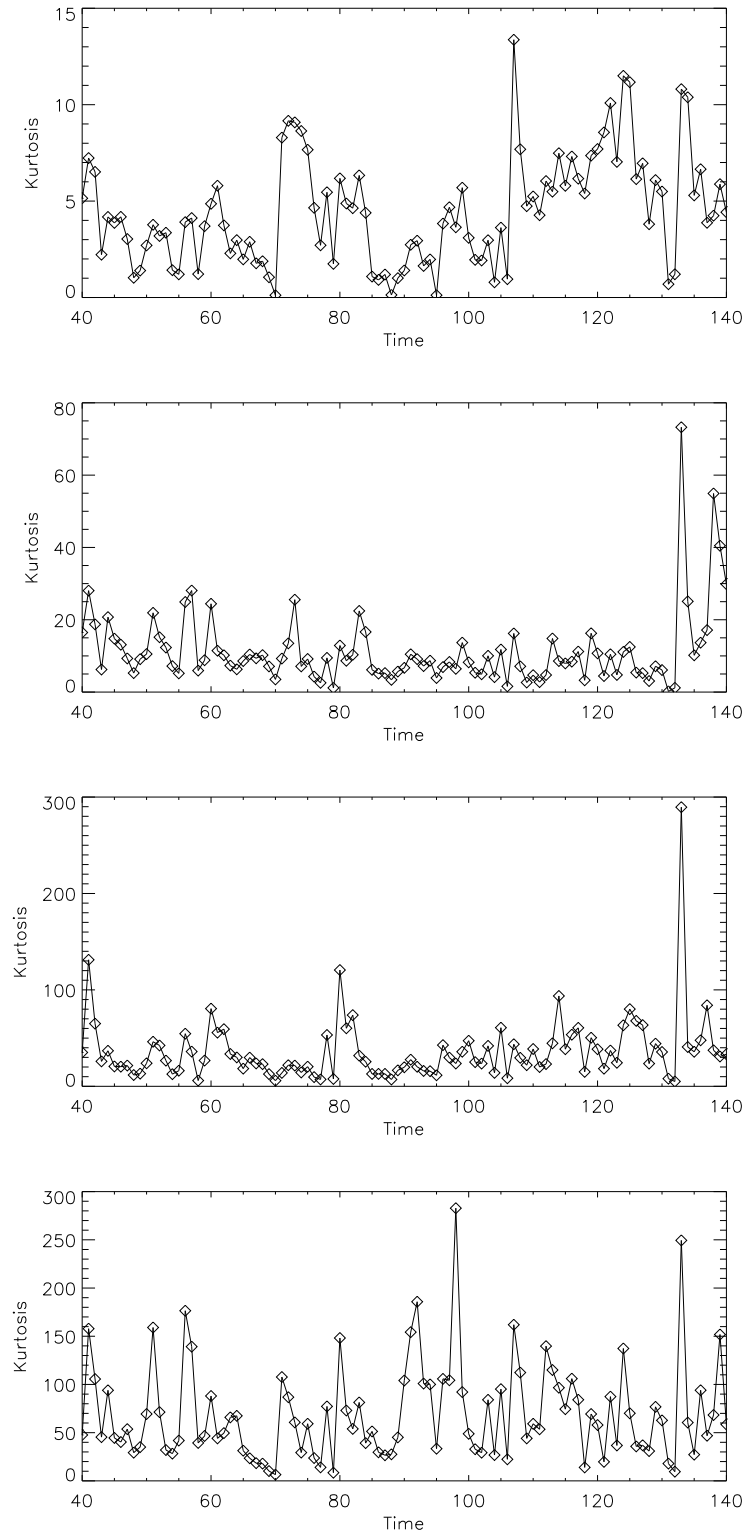


FIG. 3: Time evolution of the kurtosis of the spatial energy dissipation rate $\varepsilon(x)$ in Model A for the four different values of p used: from top to bottom $p = 0.7$, $p = 0.8$, $p = 0.9$, and $p = 1$ respectively.

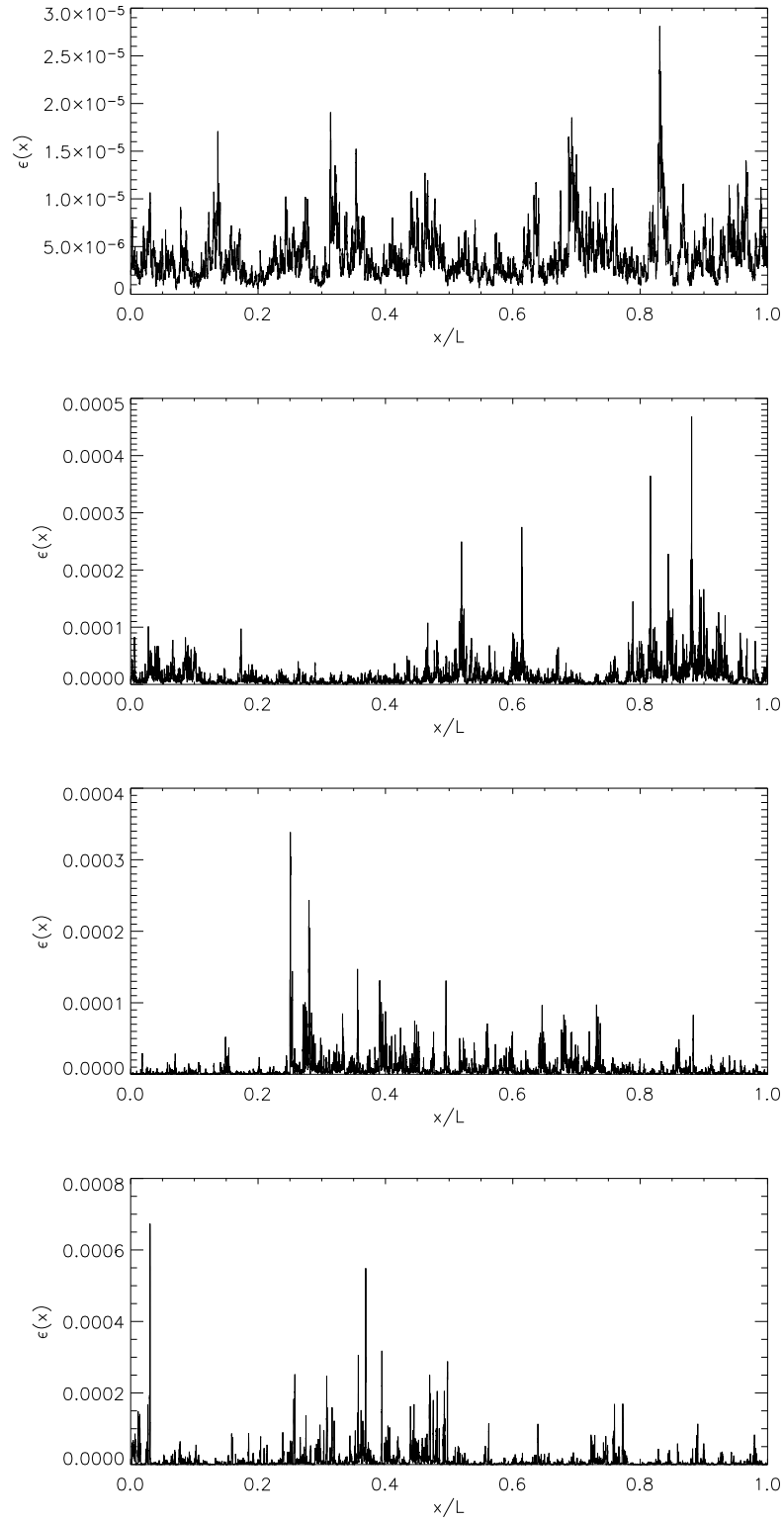


FIG. 4: Energy dissipation rate on the spatial domain in Model A: from top to bottom, $p = 0.7$ and $t = 73$, $p = 0.8$ and $t = 133$, $p = 0.9$ and $t = 80$, $p = 1$ and $t = 51$.

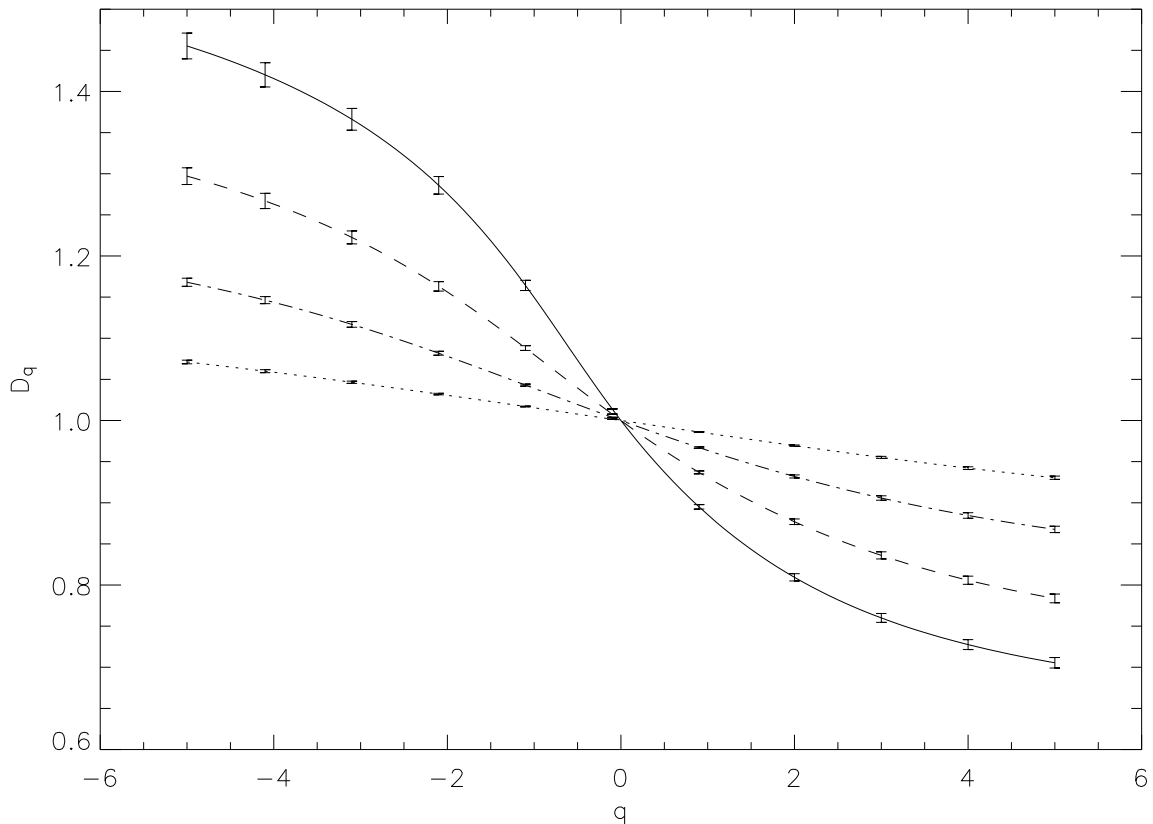


FIG. 5: Generalized dimensions D_q of the spatial energy dissipation rates in Model A for $p = 0.7$ (*Dotted line*), $p = 0.8$ (*Dash-Dotted*), $p = 0.9$ (*Dashed line*), and $p = 1.0$ (*Solid line*). The D_q values were calculated as time averages over all the time instants considered (see text). Error bars, representing standard deviation errors, are also reported for some values of q .

B. Model B

The space-time structure of the energy dissipation rate $\varepsilon(x, t)$ for $p = 0.7$ and $p = 0.8$ is shown in Fig. 6. A larger spatial fragmentation of $\varepsilon(x, t)$ for the larger p is clearly observed.

The time evolution of the kurtosis of $\varepsilon(x)$ for $p = 0.7$ and $p = 0.8$ is shown in Fig. 7. It can be seen that the typical values of the kurtosis increase going from $p = 0.7$ to $p = 0.8$ as it could be expected. Comparing Fig. 7 to Fig. 3 we can notice that, for the same p , Model B is much more intermittent than Model A. For instance, using $p = 0.8$ Model B roughly reaches the same level of intermittency as Model A with $p = 1$. In Fig. 8 we show

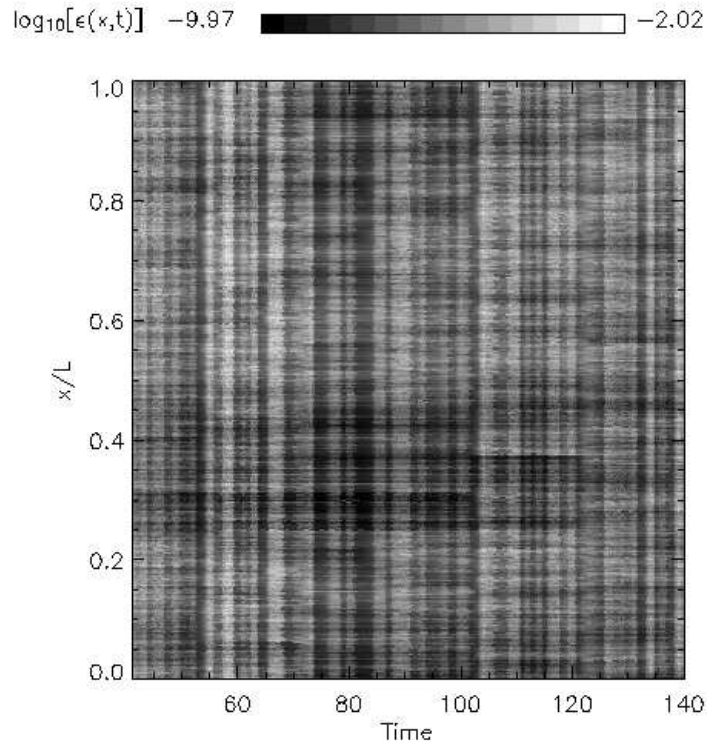
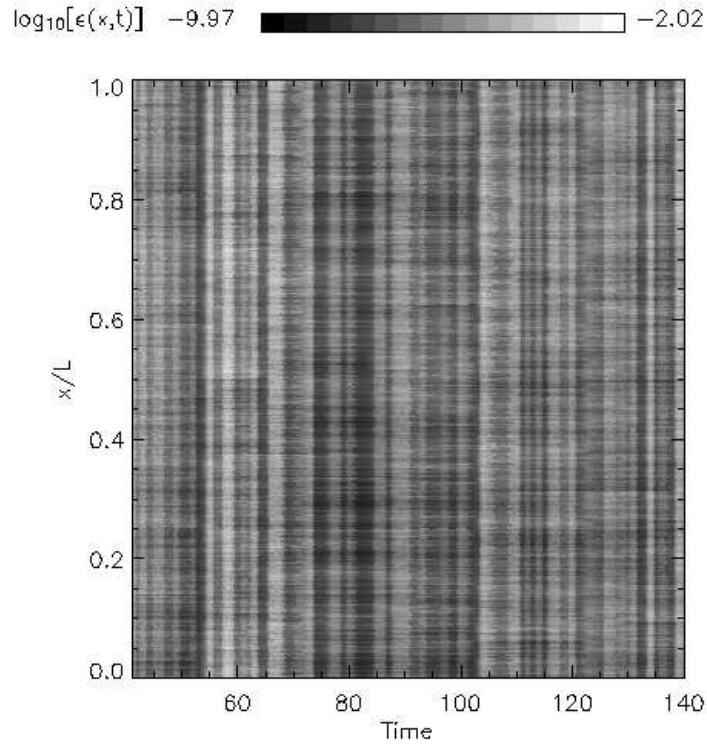


FIG. 6: Space-time structure of the energy dissipation rate $\epsilon(x,t)$ in Model B for $p = 0.7$ (top panel) and for $p = 0.8$ (bottom panel). The grey levels refer to the logarithm of $\epsilon(x,t)$.

TABLE I: Scaling exponents ζ_q for the velocity structure functions as estimated from the energy dissipation scalings in Model A for the four values of p considered. In the last column we report the velocity structure functions exponents computed from a wind tunnel experiment [37].

q	$p=0.7$	$p=0.8$	$p=0.9$	$p=1.0$	wind tunnel
1	0.337 ± 0.001	0.342 ± 0.002	0.350 ± 0.005	0.362 ± 0.008	0.37 ± 0.01
2	0.670 ± 0.001	0.675 ± 0.002	0.683 ± 0.005	0.694 ± 0.007	0.70 ± 0.01
3	1.00	1.00	1.00	1.00	1.00
4	1.326 ± 0.002	1.317 ± 0.004	1.304 ± 0.008	1.285 ± 0.012	1.28 ± 0.02
5	1.650 ± 0.005	1.628 ± 0.011	1.596 ± 0.020	1.554 ± 0.027	1.54 ± 0.03

the spatial structure of the energy dissipation rate $\varepsilon(x)$ at two time instants where a peak in the kurtosis is found, that is, $t = 58$ for $p = 0.7$ and $t = 66$ for $p = 0.8$. From this figure it is clear that also for Model B $\varepsilon(x)$ shows very strong intermittency bursts in space.

Also for Model B we investigated the spatial intermittency properties of the energy dissipation rate through the multifractal analysis described previously. The moments $\langle \mu^q \rangle$ given in Eq. (10) were calculated also in this case for $-5 \leq q \leq 5$ at the 100 time instants $t = 41, 42, \dots, 140$. Good scalings were found for all the q values and the dimensions D_q were obtained as averages over all the time instants considered. Fig. 9 shows the plot of D_q vs. q for $p = 0.7$ and $p = 0.8$. As expected, the D_q spectrum is wider for $p = 0.8$. Moreover we can observe that the D_q curve for $p = 0.8$ is very close to the one obtained in Model A for $p = 1$.

The scaling exponents ζ_q of the velocity structure functions in Model B as estimated from Eq. (12) are reported in Table II. A good agreement with the scaling exponents found in the wind tunnel experiment analyzed in Ref. [37] is obtained for $p = 0.8$.

The fact that for a given p a larger intermittency is found in Model B than in Model A is clearly a consequence of the fact that in the procedure used in Model B for the time evolution of the spatial distribution of p and $1 - p$ we consider also the local dynamics of the energy cascade as pointed out in Section III.

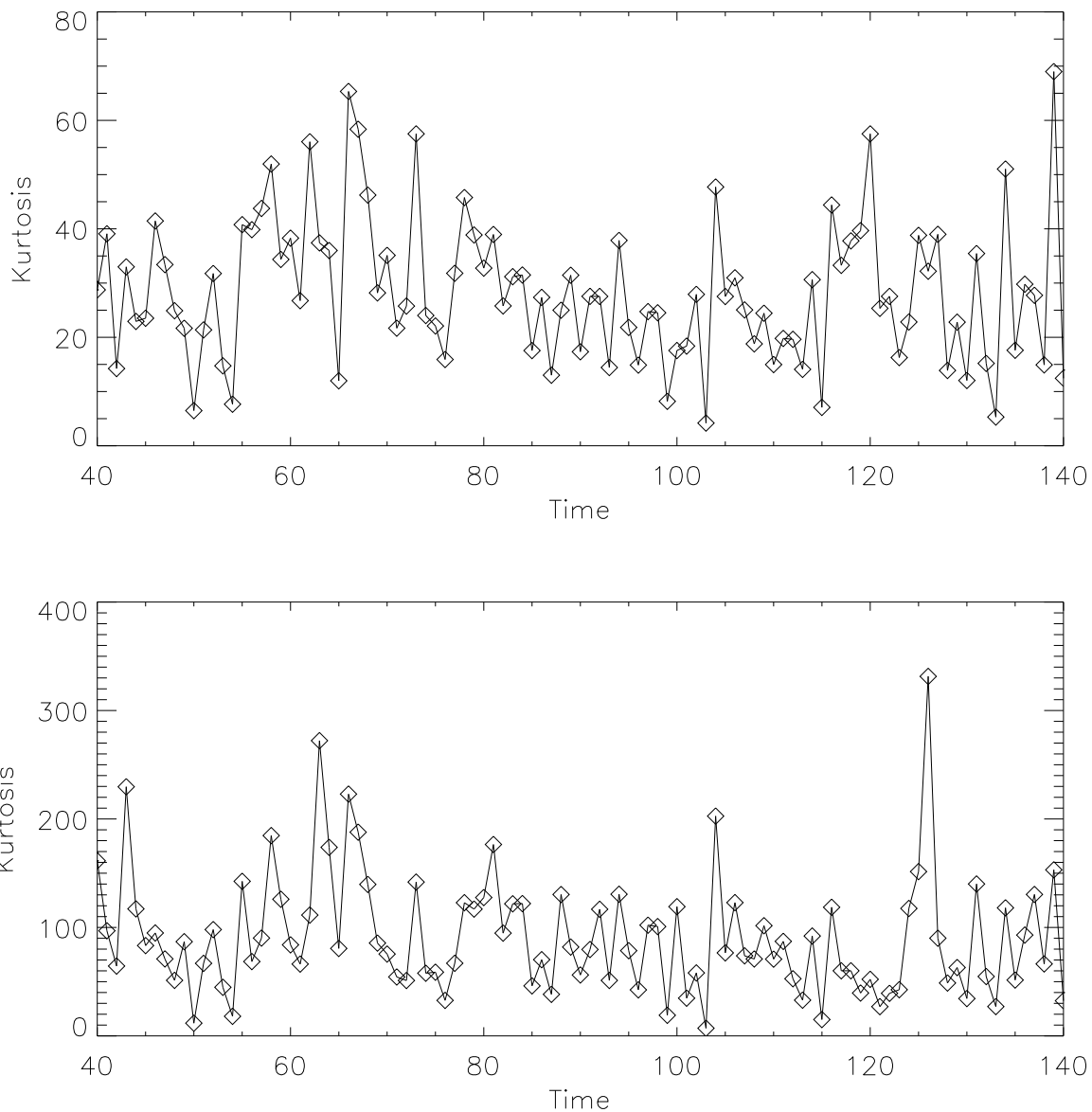


FIG. 7: Time evolution of the kurtosis of the spatial energy dissipation rate $\varepsilon(x)$ in Model B for $p = 0.7$ (top panel) and $p = 0.8$ (bottom panel).

VI. CONCLUSIONS

A problem which often arise when studying turbulent phenomena occurring in astrophysical and space fluids is the description of the intermittency of the energy dissipation process from a spatio-temporal point of view. Due to the huge Reynolds numbers occurring typically in these situations a dynamical system modeling of space-time intermittency can represent

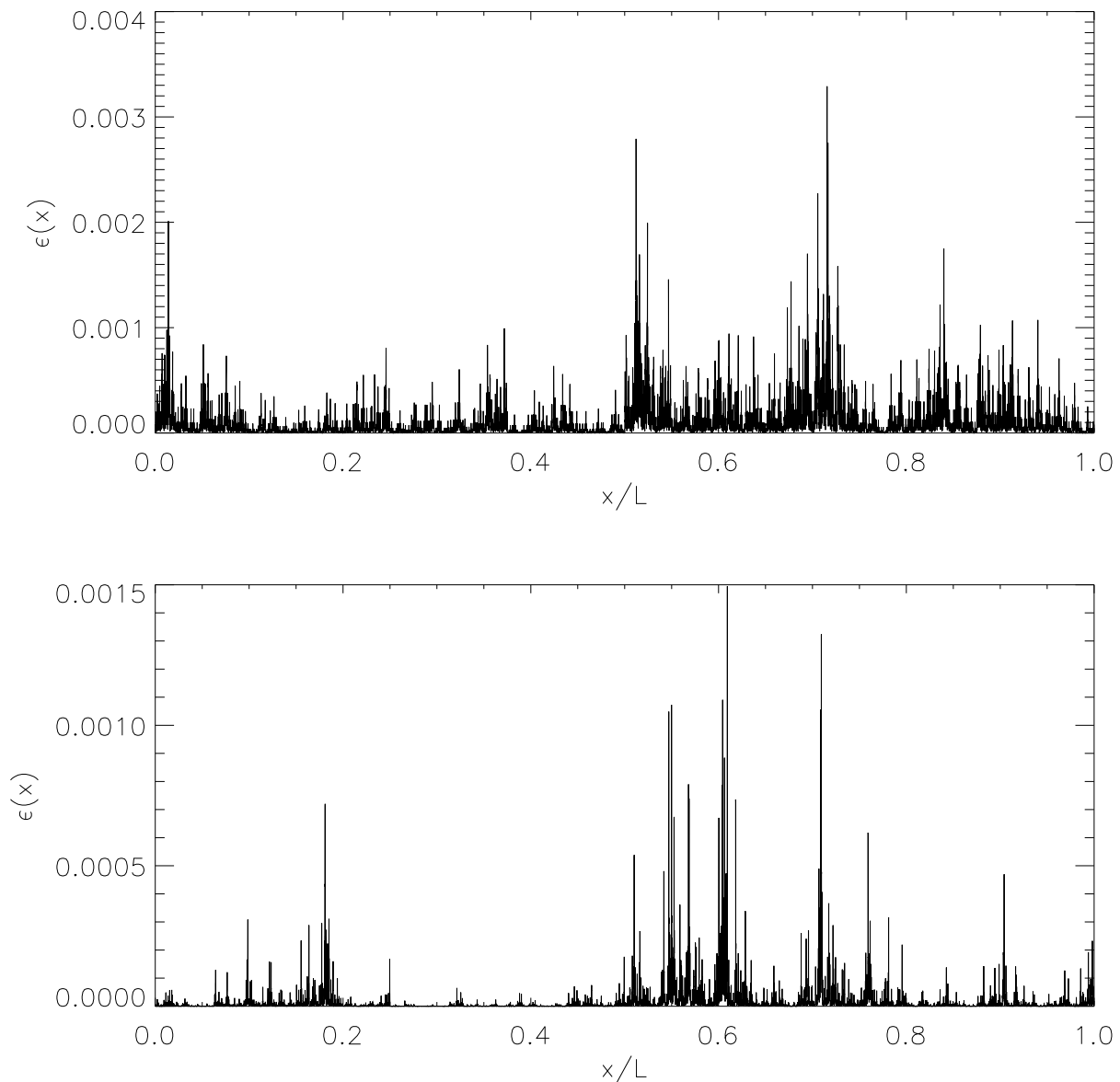


FIG. 8: Energy dissipation rate on the spatial domain in Model B for $p = 0.7$ and $t = 58$ (top panel), $p = 0.8$ and $t = 66$ (bottom panel).

an important ingredient for the characterization of such systems.

In this paper we propose a method to model the main intermittency features of energy dissipation in a turbulent system both in space and time. This is done by using a turbulence shell model and introducing some heuristic rules, partly inspired by the well known cascade p -model, to construct a spatial structure for the energy dissipation rate.

To the aim of validating the model, we performed a series of numerical simulations to

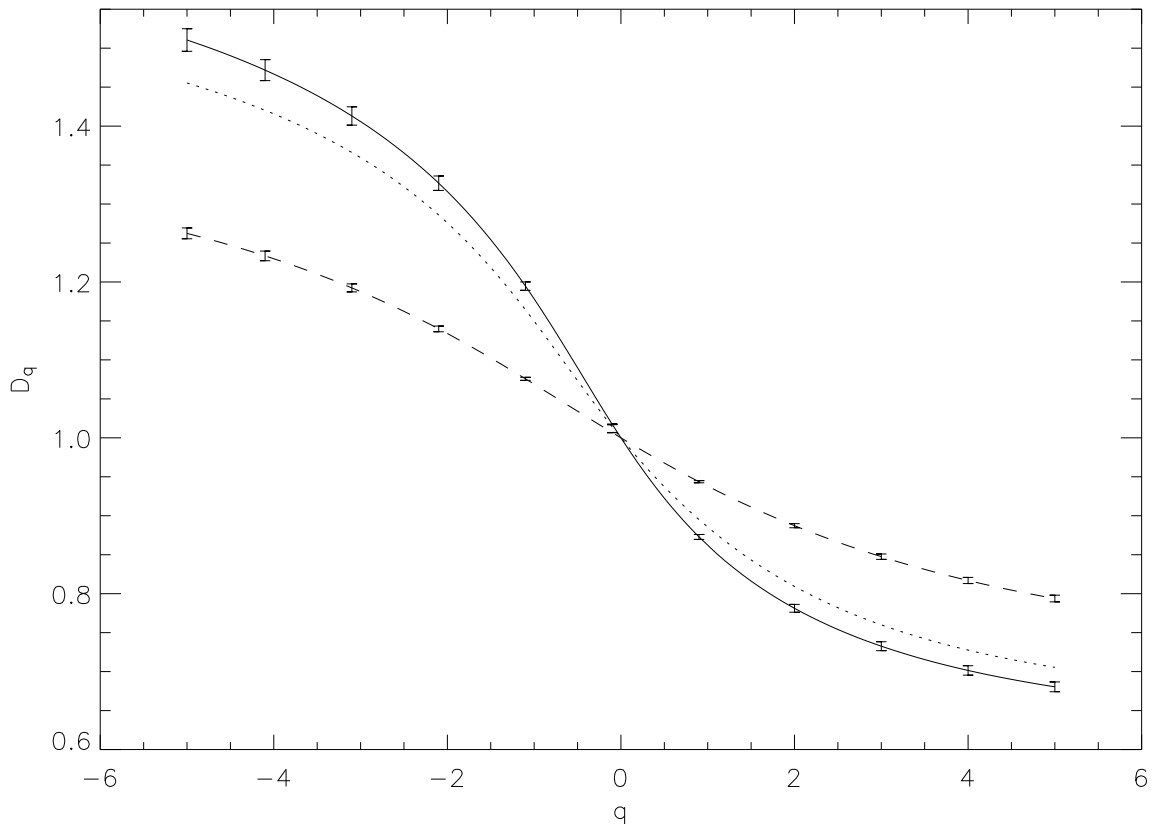


FIG. 9: Generalized dimensions D_q of the spatial energy dissipation rates in Model B for $p = 0.7$ (*Dashed line*) and $p = 0.8$ (*Solid line*). The D_q values were calculated as time averages over all the time instants considered (see text). Error bars, representing standard deviation errors, are also reported for some values of q . The D_q curve obtained in Model A for $p = 1$ is also shown as a comparison (*dotted line*).

study the spatial intermittency properties of the energy dissipation rate for different values of the free parameter p . The results show that the level of spatial intermittency of the system can be simply tuned, in both the proposed versions of the model, by changing the value of p . The spatial intermittency of the system is enhanced by increasing the p parameter. Scaling laws in agreement with those obtained in experiments involving fully turbulent hydrodynamic flows are recovered in Model A for $0.9 \lesssim p \lesssim 1$, and in Model B for $p \simeq 0.8$.

The results of this work open the way to applications of the proposed model to different physical situations. In our opinion this model could represent a useful tool to simulate

TABLE II: Scaling exponents ζ_q for the velocity structure functions as estimated from the energy dissipation scalings in Model B for $p = 0.7$ and $p = 0.8$. In the last column we report the velocity structure functions exponents computed from a wind tunnel experiment [37].

q	$p=0.7$	$p=0.8$	wind tunnel
1	0.348 ± 0.004	0.369 ± 0.009	0.37 ± 0.01
2	0.681 ± 0.004	0.700 ± 0.008	0.70 ± 0.01
3	1.00	1.00	1.00
4	1.307 ± 0.006	1.277 ± 0.014	1.28 ± 0.02
5	1.602 ± 0.015	1.536 ± 0.031	1.54 ± 0.03

the spatio-temporal intermittency of turbulent energy dissipation in those high Reynolds number astrophysical fluids where impulsive energy release processes can be associated to the dynamics of the turbulent cascade. To give just some examples, such a modeling could be interesting for studying the role of intermittent energy dissipation in the active regions of the solar corona, in the interstellar medium, and in accretion disks. We plan to investigate some of these problems in future studies.

Acknowledgments

This work was partially supported by European Commission under contract MERG-6-CT-2005-014587.

-
- [1] U. Frisch, *Turbulence: The Legacy of A.N. Kolmogorov* (Cambridge University Press, Cambridge, 1995).
 - [2] A. R. Choudhuri, *The Physics of Fluids and Plasmas* (Cambridge University Press, Cambridge, 1998).
 - [3] P. Dmitruk and D. O. Gomez, *Astrophys. J.* **484**, L83 (1997).
 - [4] P. Veltri, G. Nigro, F. Malara, V. Carbone, and A. Mangeney, *Nonlin. Proc. Geophys.* **12**, 245 (2005).

- [5] J. Franco and A. Carraminana, eds., *Interstellar Turbulence* (Cambridge University Press, Cambridge, 1999).
- [6] S. A. Balbus and J. F. Hawley, *Rev. Mod. Phys.* **70**, 1 (1998).
- [7] A. N. Kolmogorov, *Journal of Fluid Mechanics* **13**, 82 (1962).
- [8] U. Frisch, P. L. Sulem, and M. Nelkin, *Journal of Fluid Mechanics* **87**, 719 (1978).
- [9] R. Benzi, G. Paladin, G. Parisi, and A. Vulpiani, *J. Phys. A* **19**, 3771 (1984).
- [10] C. Meneveau and K. R. Sreenivasan, *Phys. Rev. Lett.* **59**, 1424 (1987).
- [11] F. Anselmetti, Y. Gagne, E. J. Hopfinger, and R. A. Antonia, *Journal of Fluid Mechanics* **140**, 63 (1984).
- [12] A. N. Kolmogorov, *Dokl. Akad. Nauk. SSSR* **30**, 301 (1941).
- [13] T. Bohr, M. H. Jensen, G. Paladin, and A. Vulpiani, *Dynamical Systems Approach to Turbulence* (Cambridge University Press, Cambridge, 1998).
- [14] P. Giuliani, *Shell Models for MHD Turbulence* (Springer-Verlag, Berlin, 1999), vol. 536 of *Lecture Notes in Physics*, p. 331.
- [15] L. Biferale, *Annu. Rev. Fluid Mech.* **35**, 441 (2003).
- [16] G. Falkovich, K. Gawedzki, and M. Vergassola, *Reviews of Modern Physics* **73**, 913 (2001).
- [17] J.-P. Laval, B. Dubrulle, and S. Nazarenko, *Physics of Fluids* **13**, 1995 (2001).
- [18] L. Chevillard, B. Castaing, E. Leveque, and A. Arneodo, *Physica D* **218**, 77 (2006).
- [19] G. Boffetta, V. Carbone, P. Giuliani, P. Veltri, and A. Vulpiani, *Phys. Rev. Lett.* **83**, 4662 (1999).
- [20] F. Lepreti, V. Carbone, P. Giuliani, L. Sorriso-Valvo, and P. Veltri, *Planetary and Space Science* **52**, 957 (2004).
- [21] G. Nigro, F. Malara, V. Carbone, and P. Veltri, *Phys. Rev. Lett.* **92**, 194501 (2004).
- [22] A. M. Obukhov, *Atmos. Oceanic Phys.* **7**, 41 (1971).
- [23] E. B. Gledzer, *Dokl. Akad. Nauk. SSSR* **208**, 1046 (1973).
- [24] V. N. Desnyansky and E. A. Novikov, *Prikl. Mat. Mekh.* **38**, 507 (1974).
- [25] M. Yamada and K. J. Ohkitani, *J. Phys. Soc. Jpn.* **56**, 4810 (1987).
- [26] M. H. Jensen, G. Paladin, and A. Vulpiani, *Phys. Rev. A* **43**, 798 (1991).
- [27] C. Gloaguen, J. Leorat, A. Pouquet, and R. Grappin, *Physica D* **17**, 154 (1985).
- [28] D. Biskamp, *Phys. Rev. E* **50**, 2702 (1994).
- [29] P. Frick and D. D. Sokoloff, *Phys. Rev. E* **57**, 4195 (1998).

- [30] P. Giuliani and V. Carbone, *Europhys. Lett.* **43**, 527 (1998).
- [31] V. S. L'vov, E. Podivilov, A. Pomyalov, I. Procaccia, and D. Vandembroucq, *Phys. Rev. E* **58**, 1811 (1998).
- [32] G. Parisi and U. Frisch, in *Turbulence and Predictability in Geophysical Fluid Dynamics*, edited by M. Ghil, R. Benzi, and G. Parisi (North-Holland, Amsterdam, 1985), p. 84, Proceed. Intern. School of Physics 'E. Fermi', Course XXXVIII, Varenna, Italy, 1983.
- [33] G. Paladin and A. Vulpiani, *Phys. Rep.* **156**, 147 (1987).
- [34] K. R. Sreenivasan, *Ann. Rev. Fluid Mech.* **23**, 539 (1991).
- [35] H. G. E. Hentschel and I. Procaccia, *Physica D* **8**, 435 (1983).
- [36] C. Meneveau and K. R. Sreenivasan, *Nucl. Phys. B (Proc. Suppl.)* **2**, 49 (1987).
- [37] G. Ruiz-Chavarria, C. Baudet, and S. Ciliberto, *Europhys. Lett.* **32**, 319 (1995).